

Grand canonical Monte Carlo simulation study of hydrogen storage by Li-decorated pha-graphene

Meng-Meng Zhang(张蒙蒙), Feng Zhang(张凤), Qiang Wu(吴强), Xin Huang(黄欣), Wei Yan(闫巍), Chun-Mei Zhao(赵春梅), Wei Chen(陈伟), Zhi-Hong Yang(杨志红), Yun-Hui Wang(王允辉), and Ting-Ting Wu(武婷婷)

Citation: Chin. Phys. B, 2023, 32 (**6**): 066803. DOI: 10.1088/1674-1056/ac8ce2
Journal homepage: http://cpb.iphy.ac.cn; http://iopscience.iop.org/cpb

What follows is a list of articles you may be interested in

A first-principles study on remote van der Waals epitaxy through a graphene monolayer on semiconductor substrates

Rui Hou(侯锐) and Shenyuan Yang(杨身园)
Chin. Phys. B, 2023, 32 (**6**): 066801. DOI: 10.1088/1674-1056/ac92d6

Rational design of Fe/Co-based diatomic catalysts for Li-S batteries by first-principles calculations

Xiaoya Zhang(张晓雅), Yingjie Cheng(程莹洁), Chunyu Zhao(赵春宇), Jingwan Gao(高敬莞), Dongxiao Kan(阚东晓), Yizhan Wang(王义展), Duo Qi(齐舵), and Yingjin Wei(魏英进)
Chin. Phys. B, 2023, 32 (**3**): 036803. DOI: 10.1088/1674-1056/aca6da

First principles study of hafnium intercalation between graphene and Ir(111) substrate

Hao Peng(彭浩), Xin Jin(金鑫), Yang Song(宋洋), and Shixuan Du(杜世萱)
Chin. Phys. B, 2022, 31 (**10**): 106801. DOI: 10.1088/1674-1056/ac6941

Effects of oxygen concentration and irradiation defects on the oxidation corrosion of body-centered-cubic iron surfaces: A first-principles study

Zhiqiang Ye(叶志强), Yawei Lei(雷亚威), Jingdan Zhang(张静丹), Yange Zhang(张艳革), Xiangyan Li(李祥艳), Yichun Xu(许依春), Xuebang Wu(吴学邦), C. S. Liu(刘长松), Ting Hao(郝汀), and Zhiguang Wang(王志光)
Chin. Phys. B, 2022, 31 (**8**): 086802. DOI: 10.1088/1674-1056/ac633c

Sodium decorated net-Y nanosheet for hydrogen storage and adsorption mechanism: A first-principles study

Yunlei Wang(王云蕾), Yuhong Chen(陈玉红), Yunhui Wang(王允辉)
Chin. Phys. B, 2020, 29 (**1**): 016801. DOI: 10.1088/1674-1056/ab5785

Grand canonical Monte Carlo simulation study of hydrogen storage by Li-decorated pha-graphene

Meng-Meng Zhang(张蒙蒙)[1], Feng Zhang(张凤)[1], Qiang Wu(吴强)[2], Xin Huang(黄欣)[1], Wei Yan(闫巍)[1], Chun-Mei Zhao(赵春梅)[1], Wei Chen(陈伟)[1], Zhi-Hong Yang(杨志红)[1], Yun-Hui Wang(王允辉)[1,†], and Ting-Ting Wu(武婷婷)[1,‡]

[1] *College of Science, Nanjing University of Posts and Telecommunications, Nanjing* 210023, *China*
[2] *College of Electronic and Optical Engineering and College of Flexible Electronics (Future Technology), Nanjing University of Posts and Telecommunications, Nanjing* 210023, *China*

(Received 5 June 2022; revised manuscript received 4 August 2022; accepted manuscript online 26 August 2022)

Grand canonical Monte Carlo simulation (GCMCs) is utilized for studying hydrogen storage gravimetric density by pha-graphene at different metal densities, temperatures and pressures. It is demonstrated that the optimum adsorbent location for Li atoms is the center of the seven-membered ring of pha-graphene. The binding energy of Li-decorated pha-graphene is larger than the cohesive energy of Li atoms, implying that Li can be distributed on the surface of pha-graphene without forming metal clusters. We fitted the force field parameters of Li and C atoms at different positions and performed GCMCs to study the absorption capacity of H_2. The capacity of hydrogen storage was studied by the differing density of Li decoration. The maximum hydrogen storage capacity of 4Li-decorated pha-graphene was 15.88 wt% at 77 K and 100 bar. The enthalpy values of adsorption at the three densities are in the ideal range of 15 kJ·mol^{-1}–25 kJ·mol^{-1}. The GCMC results at different pressures and temperatures show that with the increase in Li decorative density, the hydrogen storage gravimetric ratio of pha-graphene decreases but can reach the 2025 US Department of Energy's standard (5.5 wt%). Therefore, pha-graphene is considered to be a potential hydrogen storage material.

Keywords: hydrogen storage, pha-graphene, grand canonical Monte Carlo simulation (GCMCs), force field

PACS: 68.43.Bc, 31.15.E–, 02.70.Tt, 73.20.At **DOI:** 10.1088/1674-1056/ac8ce2

1. Introduction

With the rapid growth in energy demand and massive burning of fossil fuels, it is imperative to develop and utilize clean and renewable resources. Hydrogen (H_2) stands out in this field due to its high calorific value (144 mJ·kg^{-1}) and excellent mass–energy density.[1] Wind, solar and other forms of clean energy are random and intermittent. Their large-scale and base development modes pose technical and economic challenges for wind power and other clean energy in China at the initial stage of development. However, due to the low gravimetric density of adsorbed hydrogen at room temperature, its storage performance is still far from meeting the US Department of Energy's (DOE's) ultimate goal.

At present, hydrogen storage methods mainly include gas, liquid and solid hydrogen storage.[2–6] Storage of hydrogen gas requires high-pressure tanks, which have a low gravimetric density and poor safety.[7] Liquid hydrogen storage has some disadvantages, such as high energy consumption, high cost and troublesome operating conditions.[7] In addition to these storage methods, extensive research has been made into a reversible, safe technique for solid-state storage by physical or chemical methods.[8] The chemical process of physical adsorption of hydrogen molecules through hydrogen storage materials involves the reaction of a hydrogen storage substance with a hydrogen molecule. These methods should meet DOE goals such as high hydrogen storage density, reversible hydrogen storage and release of hydrogen under environmental conditions.[9] In recent years, solid hydrogen storage materials have been widely studied and show excellent hydrogen storage performance. Solid hydrogen storage appears to be the best among the three kinds of hydrogen storage methods, and is at the forefront of research. Therefore, it is very important to find high-quality hydrogen storage materials, and this would be conducive to breaking through the bottleneck of hydrogen energy development.

The US DOE requires domestic on-board hydrogen batteries to have a hydrogen gravimetric density (the ratio of hydrogen released to total hydrogen gravimetric) of 5.5 wt% by 2025, with an eventual goal of 6.5 wt%. For suitable hydrogen adsorption and desorption processes, the average binding energy at room temperature is 0.2 eV/H_2–0.6 eV/H_2.[10] In addition, the selected host material has a high surface area and is light in weight. To achieve these goals, carbon-based nanomaterials are a better choice for hydrogen storage[11,12] (e.g., carbon nanotubes,[13] fullerenes,[14] graphene,[15] etc.). Pure graphene sheets have poor hydrogen storage performance because they do not have suitable adsorption sites for hydrogen molecules.[16] One of the reported strategies for improving the

†Corresponding author. E-mail: yhwang@njupt.edu.cn
‡Corresponding author. E-mail: wutt@njupt.edu.cn

© 2023 Chinese Physical Society and IOP Publishing Ltd

hydrogen storage performance of graphene-based materials is to modify them with metal atoms, which change the surface state of the material and can be used as effective adsorption sites for hydrogen molecules and exhibit good hydrogen storage performance.[17–20] Recently, Shi *et al.* observed that the maximum hydrogen storage performance of Li-modified net-τ reached 13.29 wt%.[21]

Recently, a new two-dimensional carbon-based material, pha-graphene,[22] has been proposed. It is an antisymmetric graphene allotrope consisting of three carbon rings containing five, six and seven carbon atoms. The energy, dynamic and thermal stability of the structure are fully confirmed.[23,24] Monte Carlo (MC) simulation based on probability and statistics theory was proposed by Von Neumann and colleagues in the 1940s. As an important numerical calculation method, MC simulation has been widely used in the study of the thermodynamic and kinetic properties of ionic conductors.[25–27] By the 1950s, the Metropolis algorithm,[28] which can be applied to most physical equilibrium systems in MC simulation, was proposed. According to different research objects, MC simulation can be divided into two categories: one is the simulation of non-time correlation of the thermodynamic equilibrium process, such as the common grand canonical Monte Carlo simulation (GCMCs) while the other is the study of time-dependent dynamical problems, such as the kinetic Monte Carlo (KMC) simulation. The ultimate goal of both MC simulations is to find the configuration of structures hovering near a low potential energy surface as much as possible. As a classical thermodynamic MC simulation, GCMCs is widely used in the synthesis and porous adsorption of electrochemical energy storage materials. In recent years, hydrogen storage materials based on first-principles calculations have made some progress.[29–33] Based on density functional theory (DFT) and GCMCs, the hydrogen storage performance of Li-decorated pha-graphene has been studied theoretically. The results show that Li atoms tend to adsorb at P_3 because the maximum binding energy is at P_3. In this paper, the hydrogen storage performance of pha-graphene decorated with different densities of Li at different temperatures and pressures was studied by GCMCs. The simulation results show that pha-graphene is a potential hydrogen storage material.

2. Computational details

In this paper, the capacity of Li-decorated pha-graphene was explored based on DFT.[34] The generalized gradient approximation (GGA) formulated by the Perdew–Burke–Ernzerhof functional is used for structure and energy optimization.[35] The DFT-D2 method of Grime is used to describe the van der Waals interaction.[36] The k-point of the Brillouin zone is set to $6\times6\times1$, and the cutoff energy is 500 eV. In order to ensure the accuracy of the calculation, the relaxation convergence criteria of energy and force are set to 10^{-5} eV and 0.01 eV·Å^{-1}, respectively. The vacuum layer thickness is set to 20 Å to prevent interlayer interaction.

The average binding energy of Li atoms decorated on a pha-graphene surface at different densities can be expressed as

$$E_{\mathrm{b}}=\frac{E_{m\mathrm{Li+pha\text{-}graphene}}-mE_{\mathrm{Li}}-E_{\mathrm{pha\text{-}graphene}}}{m},$$

where m represents the number of Li atoms, E_{Li}, $E_{\mathrm{pha\text{-}graphene}}$ and $E_{m\mathrm{Li+pha\text{-}graphene}}$ represent the energy of a single Li atom, the pha-graphene primitive cell total energy and the pha-graphene primitive cell total energy when decorated by Li atoms, respectively. The hydrogen storage gravimetric density of the system is defined as

$$G(\mathrm{wt\%})=\frac{nM_{\mathrm{H_2}}}{nM_{\mathrm{H_2}}+M_{m\mathrm{Li+pha\text{-}graphene}}}\times100\%,$$

wherein $M_{\mathrm{H_2}}$ and $M_{m\mathrm{Li+pha\text{-}graphene}}$ represent the relative molecular weight of a single $M_{\mathrm{H_2}}$ molecule and the total relative molecular weight of m a pha-graphene system decorated with Li atoms, respectively.

GCMCs obtains the hydrogen storage gravimetric density curve and adsorption enthalpy curve of hydrogen. Under the condition that the chemical potential, volume and temperature of hydrogen molecules remain unchanged, the Metropolis importance sampling algorithm is adopted, and the Ewald method is adopted for electrostatic interaction. Both the balance and production steps are set to 5×10^6. According to the structure of the paper, the force field parameters of Dreiding were modified, and hydrogen adsorption was carried out at a fixed temperature and different pressures. Based on the following understanding, 77 K (−196 °C) is the lowest temperature that can be achieved in the current experiment and 233 K (−40 °C) is the lower limit of near-ambient temperature set by the DOE. Furthermore, 298 K (25°C) is used for the simulation at room temperature. Therefore, the hydrogen adsorption data were measured at these three fixed temperatures of 77 K, 233 K, and 298 K and at control pressures of 1 bar–100 bar, respectively.

3. Results and discussion

Figure 1 shows the top and side views of the optimized primitive cell and the pha-graphene decorated with different Li densities. As can be seen in Fig. 1(a), the four possible adsorption sites are P_1 (the center of a five-membered ring), P_2 (the center of a six-membered ring), P_3 (the center of a seven-membered ring) and P_4 (the center of the lower six-membered ring). Cohesive energy is defined as the difference between the compound energy and the sum of the corresponding isolated atomic energy.[37–39] The experimental cohesive energy

of Li atoms is 1.63 eV.[40] The average binding energies of a single Li atom at P_1, P_2, P_3 and P_4 are −2.40 eV, −2.47 eV, −2.51 eV and −2.45 eV, respectively.

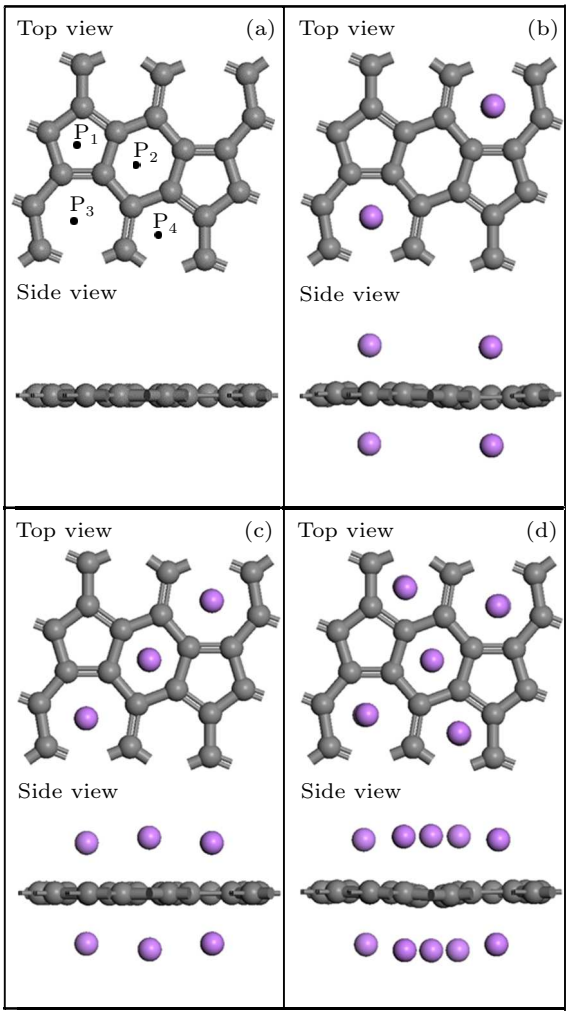


Fig. 1. Views of the optimized structure from above and from the sides: (a) optimized unit cell of pha-graphene, (b) 4Li-decorated pha-graphene, (c) 6Li-decorated pha-graphene and (d) 10Li-decorated pha-graphene. The dotted lines present a primitive cell. The gray and purple spheres represent C and Li atoms, respectively.

We found that the binding energies of these four sites were P_3, P_2, P_4 and P_1 from large to small, which were all greater than the cohesive energy of Li atoms, indicating that metal aggregation would not occur. We also found that the binding energy difference between the optimal adsorption site P_3 and the secondary P_2 and tertiary P_4 adsorption sites was slight. Therefore, we considered decorating the optimal adsorption position and symmetric position with Li atoms first and then modifying the secondary and tertiary adsorption positions with Li atoms successively. Eventually, 4, 6 and 10 Li atoms were introduced. The optimized structures are exhibited in Figs. 1(b)–1(d). It can be observed that the Li atoms in the three optimized metal density Li-modified structures are symmetrically distributed on both sides of pha-graphene. With increase in the density of Li metal, the distribution of Li atoms is different from that of 4Li-decorated pha-graphene distributed in parallel on both sides, but presents a certain curvature. The average binding energies of single Li atoms of pha-graphene decorated with 4Li, 6Li and 10Li are −2.02 eV, −1.94 eV and −1.96 eV, respectively. The average binding energy of Li at the three densities is greater than the cohesive energy of Li atoms (1.63 eV) obtained in the experiment. It can be found that with the increase in Li density, the average binding energy of Li atoms first decreases and then becomes constant at a certain point (6Li here), but the average binding energy between Li atoms and the pha-graphene is greater than the cohesive energy of Li atoms obtained experimentally, so metal agglomerations will not be formed. However, when 14Li atoms are considered for decoration, it is found that the optimized structure is no longer stable. The average adsorption energy decreases the density with the increase in Li. This suggests that Li atoms cannot grow indefinitely.

GCMCs explored the H_2 adsorption isotherms and adsorption enthalpy change curves of pha-graphene decorated by 4Li, 6Li and 10Li in the pressure range of 0–100 bar and at fixed temperatures of 77 K, 233 K and 298 K. Force field parameters of the interaction of H_2 with Li-decorated pha-graphene can be obtained by fitting the Morse equation

$$U(r_{ij}) = D\left\{\exp\left[\alpha\left(1-\frac{r_{ij}}{r_0}\right)\right] - 2\times\exp\left[\frac{\alpha}{2}\left(1-\frac{r_{ij}}{r_0}\right)\right]\right\},$$

where r_{ij}, D, α and r_0 denote the interaction distance, well depth, force constant and the equilibrium bond distance, respectively. The optimal adsorption potential energy of the interaction of H_2 and Li-decorated pha-graphene calculated by DFT simulation and the fitted potential energy curve is shown in Fig. 2. It can be seen that the fitting curve is completely consistent with the results of the DFT calculation. The Morse force field parameters are shown in Table 1. Here Li_4, Li_5 and Li_6 represent the atomic types of Li and are located at the best P_3, P_2 and P_4 positions, respectively. C_7, C_6 and C_5 represent the types of C atoms in the corresponding rings of P_3, P_2 and P_4. Other field parameters of C atoms in pha-graphene were taken from the Dreiding field.[41]

Table 1. The Morse potential force field parameters employed in this paper.

Term	D (eV)	r_0 (Å)	α
Li_4–H_A	0.11105	2.03219	7.01532
Li_5–H_A	0.11283	2.03128	6.98927
Li_6–H_A	0.11183	2.03583	7.00256
C_7–H_A	0.09723	3.45697	5.65769
C_6–H_A	0.10265	3.43157	5.61142
C_5–H_A	0.10227	3.42287	5.66535

The H_2 adsorption isotherms of pha-graphene decorated with Li of different densities are shown in Fig. 3 for increasing pressure. According to the adsorption isotherm in Fig. 3, it can be concluded that when the pressure of 4Li- and 6Li-decorated pha-graphene is greater than 30 bar and 50 bar, respectively,

the hydrogen storage gravimetric ratio at all three temperatures exceeds 5.5 wt% (2025 DOE standard). The maximum hydrogen storage gravimetric ratio reaches 15.88 wt% and 14.65 wt% at 77 K and 100 bar, respectively. However, the maximum hydrogen storage gravimetric ratio of the 10Li-decorated pha-graphene isotherm is only 5.3 wt% at a pressure of 100 bar and temperature of 298 K. Longitudinal comparison of adsorption isotherms under the three densities shows that the lower the temperature is, the higher the hydrogen storage is under the condition of fixed pressure. From the GCMCs data of pha-graphene decorated with different Li densities, under the same conditions, the hydrogen storage gravimetric ratio of pha-graphene decreases with increase in the metal Li density. The reason for this phenomenon is that with the increase in modification density, the effective adsorption sites of hydrogen do not increase but become fewer and fewer, resulting in a decrease in the hydrogen storage gravimetric ratio. This can also be seen from the diagram of maximum hydrogen storage density in Fig. 3(a).

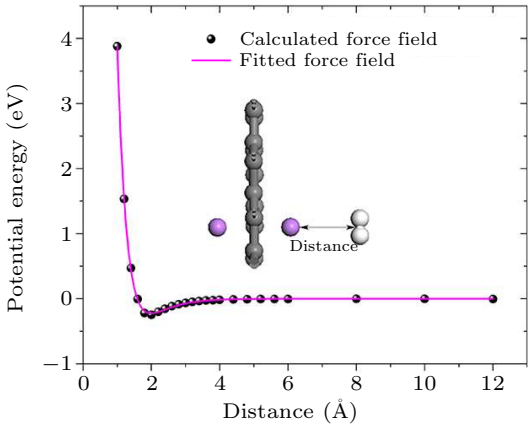


Fig. 2. DFT calculation of H_2 and Li-decorated pha-graphene and comparison of the fitting force field. The white, purple and gray spheres represent H, Li and C atoms, respectively.

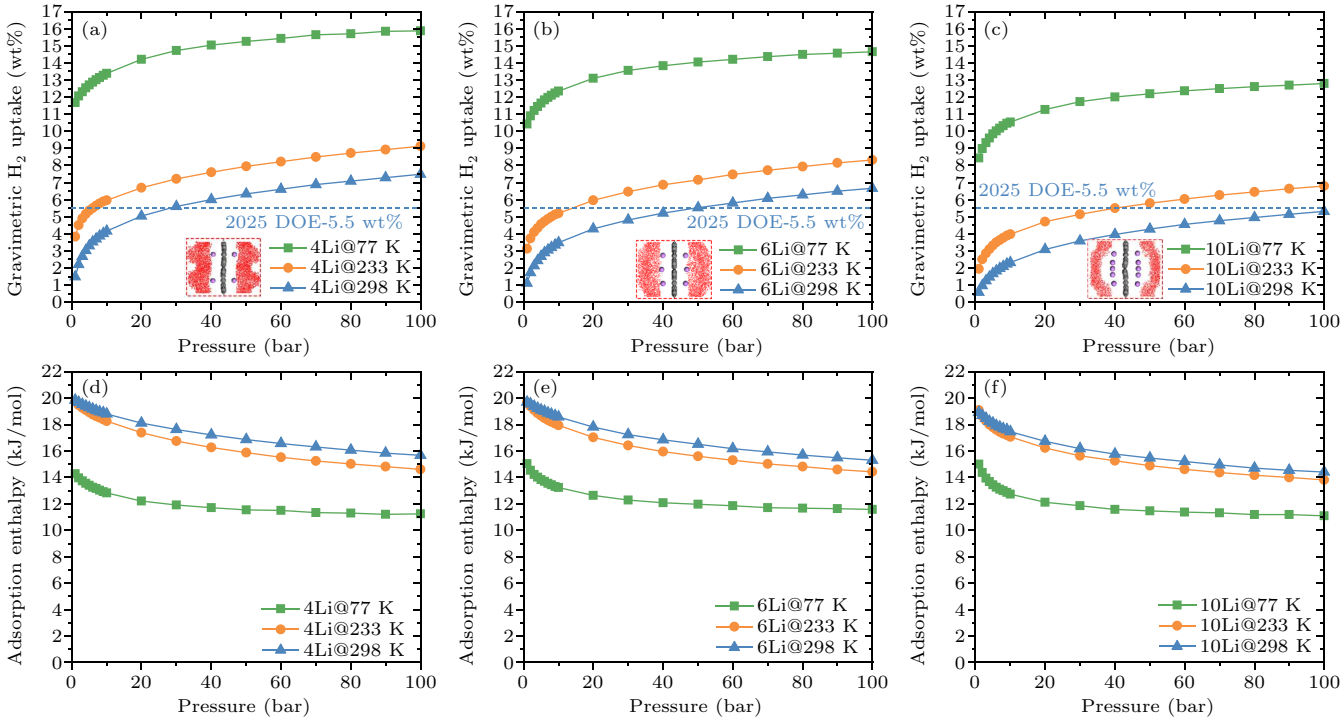


Fig. 3. The gravimetric adsorption isotherms of H_2 calculated for pha-graphene decorated with different Li densities and the adsorption enthalpy at 77 K, 233 K and 298 K in the range from 1 bar to 100 bar: (a) 4Li-decorated gravimetric hydrogen adsorption isotherms, (b) 6Li-decorated gravimetric hydrogen adsorption isotherms, (c) 10Li-decorated gravimetric hydrogen adsorption isotherms, (d) 4Li-decorated enthalpy of adsorption, (e) 6Li-decorated enthalpy of adsorption, (f) 10Li-decorated enthalpy of adsorption, The blue, orange and green solid lines correspond to 298 K, 233 K and 77 K, respectively, while the blue dotted line represents the 2025 DOE standard. The illustrations in (a)–(c) are snapshots of hydrogen adsorption density at corresponding densities at 77 K and 100 bar.

Adsorption enthalpy is used to measure the strength of the interaction between H_2 and adsorbent surfaces or pore structures. Therefore, the change in adsorption enthalpy from 1 bar to 100 bar at different temperatures and densities is shown in the second row of Fig. 3. It can be seen from the horizontal comparison that the overall trend of adsorption enthalpy at three temperatures and three densities is slowly decreasing, which is the same as the change trend reported previously. GCMCs results show that the adsorption enthalpy values for different decoration densities, temperatures and pressures are in the ideal range of adsorption enthalpy (15 kJ·mol^{-1}–25 kJ·mol^{-1}).[42] The results for adsorption enthalpy obtained by GCMCs are in agreement with recent research results.[21,43–45] It can also be concluded from the change curve of adsorption enthalpy that, at fixed temperature, the adsorption enthalpy decreases gradually with an increase in pressure. At fixed pressure, as the temperature increases, the binding energy of hydrogen molecules will de-

crease and the hydrogen storage gravimetric ratio will also decrease. Therefore, we can promote the release of adsorbed hydrogen molecules by increasing the temperature so as to realize hydrogen energy utilization. In summary, GCMCs suggest that pha-graphene is a promising candidate for hydrogen storage.

4. Conclusion

In this paper we fitted the field parameters of Li and C atoms. The GCMCs method was used to evaluate the hydrogen storage capacity of pha-graphene decorated with different Li densities at different temperatures and pressures. First, we constructed three hydrogen adsorption structures by Li atom decoration. Second, we discussed the effect of modification of different Li atomic density on the hydrogen storage performance of pha-graphene by adsorption isotherm and adsorption enthalpy curves. The GCMCs results show that the hydrogen storage capacity of 4Li-decorated pha-graphene was proved to be 7.49 wt%, 9.12 wt% and 15.88 wt% at 298 K, 233 K and 77 K, respectively. The hydrogen storage capacities of 6Li-decorated pha-graphene are 6.67 wt%, 8.32 wt% and 14.65 wt% at 298 K, 233 K and 77 K, respectively. The hydrogen storage capacities of 10Li-decorated pha-graphene are 5.31 wt%, 6.79 wt% and 12.79 wt% at 298 K, 233 K and 77 K, respectively. All GCMCs results show that Li-decorated pha-graphene can be used as a candidate material for hydrogen storage materials.

Acknowledgments

Project supported by the National Natural Science Foundation of China (Grant Nos. 11904175, 11804169, and 11804165) and the Graduate Innovation Project of Jiangsu Province, China (Grant No. KYCX21_0700).

References

[1] Jain V and Kandasubramanian B 2020 *J. Mater. Sci.* **55** 1865
[2] Ouyang L, Liu F, Wang H, Liu J W, Yang X S, Sun L X and Zhu M 2020 *J. Alloys Compd.* **832** 154865
[3] AbdKhalim Khafidz N Z, Yaakob Z, Lim K L and Timmiati S N 2016 *Int. J. Hydrog. Energy* **41** 13131
[4] Rusman N and Dahari M 2016 *Int. J. Hydrog. Energy* **41** 12108
[5] Gangu K K, Maddila S, Mukkamala S B and Jonnalagadda S B 2019 *J. Energy Chem.* **30** 132
[6] Moradi R and Groth K M 2019 *Int. J. Hydrog. Energy* **44** 12254
[7] Sakintuna B, Lamari-Darkrim F and Hirscher M 2007 *Int. J. Hydrog* **32** 1121
[8] Walker G 2008 1-*Hydrogen storage technologies* (Woodhead Publishing) pp. 3–17
[9] Broom D P 2011 *Hydrogen Sorption Properties of Materials* (London: Springer London) pp. 61–115
[10] Kim Y H, Zhao Y, Williamson A, Heben M J and Zhang S B 2006 *Phys. Rev. Lett.* **96** 016102
[11] Xia Y, Yang Z and Zhu Y 2013 *J. Mater. Chem. A* **1** 9365
[12] Jastrzębski K and Kula P 2021 *Materials* **14** 10
[13] Dillon A C, Jones K M, Bekkedahl T A, Kiang C H, Bethune D S and Heben M J 1997 *Nature* **386** 377
[14] Ren H, Cui C, Li X and Liu Y 2017 *Int. J. Hydrog. Energy* **42** 312
[15] Wang Y, Wu Q, Deng S, Ma R, Huang X, Bi L and Yang Z 2019 *Appl. Surf. Sci.* **495** 143621
[16] Yang S, Liu Y, Shi Q, Zou J and Yang H 2018 *J. Orthop. Translat.* **12** 1
[17] Zhang F C, Liu Y and Zhang W B 2015 *Chin. Phys. Lett.* **32** 057302
[18] Xiao-Feng Z, Hao-Yu F and Chun-Mei T 2019 *Acta Phys. Sin.* **68** 053601 (in Chinese)
[19] Sui P, Dai J, Zhao Y and Dai Z 2018 *Chin. Phys. B* **27** 097311
[20] Zhang C, Tang S, Deng M and Du Y 2018 *Chin. Phys. B* **27** 066103
[21] Shi M, Wu Q, Huang X, Meng Z, Wang Y, Yang Z, Hu J, Xu Y, Zhao H and Yan G 2021 *Int. J. Hydrog. Energy* **46** 21965
[22] Wang Z, Zhou X F, Zhang X, Zhu Q, Dong H, Zhao M and Oganov A R 2015 *Nano Lett.* **15** 6182
[23] Shirazi A H N 2019 *Front. Struct. Civ. Eng.* **13** 495
[24] Shekaari A and Jafari M 2022 *Mol. Simul.* **48** 712
[25] Moon J, Lee B, Cho M and Cho K 2014 *J. Power Sources* **272** 1010
[26] Lv D, Wang W, Liu J P, Guo D Q and Li S X 2018 *J. Magn. Magn. Mater.* **465** 348
[27] Kar P and Harinipriya S 2014 *J. Electrochem. Soc.* **161** A726
[28] Metropolis N and Ulam S 1949 *J. Am. Stat Assoc.* **44** 335
[29] Xu B, Wang Y S, Song N H, Zhang J, Li M and Yi L 2016 *Chin. Phys. Lett.* **33** 016802
[30] Zhang F C, Liu Y and Zhang W B 2015 *Chin. Phys. Lett.* **32** 057302
[31] Wang X Q, Wang Y S, Wang Y C, Wang F, Sun Q and Jia Y 2014 *Chin. Phys. Lett.* **31** 026801
[32] Luo X F, Fang C, Li X, Lai W S, Sun L F and Liang T X 2013 *Chin. Phys. Lett.* **30** 066801
[33] Wang Y, Chen Y and Wang Y 2020 *Chin. Phys. B* **29** 016801
[34] Kresse G and Furthmüller J 1996 *Phys. Rev. B* **54** 11169
[35] Perdew J P, Burke K and Ernzerhof M 1996 *Phys. Rev. Lett.* **77** 3865
[36] Grimme S 2006 *J. Comput. Chem.* **27** 1787
[37] Ding Y and Wang Y 2015 *Nanoscale Res. Lett.* **10** 13
[38] Bai H, Zhu Y, Qiao W and Huang Y 2011 *RSC Adv.* **1** 768
[39] Zhu Y, Bai H and Huang Y 2016 *J. Phys.: Condens. Matter* **28** 045303
[40] Chan K T, Neaton J B and Cohen M L 2008 *Phys. Rev. B* **77** 235430
[41] Mayo S L, Olafson B D and Goddard W A 1990 *J. Phys. Chem. C* **94** 8897
[42] Bhatia S K and Myers A L 2006 *Langmuir* **22** 1688
[43] Bi L, Yin J, Huang X, Wang Y and Yang Z 2020 *Int. J. Hydrog. Energy* **45** 17637
[44] Wang Y, Xu G, Deng S, Wu Q, Meng Z, Huang X, Bi L, Yang Z and Lu R 2020 *Appl. Surf. Sci.* **509** 144855
[45] Shi M, Bi L, Huang X, Meng Z, Wang Y and Yang Z 2020 *Appl. Surf. Sci.* **534** 147606